

Evidence of a Precursor Superconducting Phase at Temperatures as High as 180 K in $\text{RBa}_2\text{Cu}_3\text{O}_{7-\delta}$ ($R = \text{Y, Gd, Eu}$) Superconducting Crystals from Infrared Spectroscopy

A. Dubroka,¹ M. Rössle,¹ K. W. Kim,¹ V. K. Malik,¹ D. Munzar,² D. N. Basov,³ A. A. Schafgans,³ S. J. Moon,³ C. T. Lin,⁴ D. Haug,⁴ V. Hinkov,⁴ B. Keimer,⁴ Th. Wolf,⁵ J. G. Storey,⁶ J. L. Tallon,⁶ and C. Bernhard^{1,*}

¹University of Fribourg, Department of Physics and Fribourg Center for Nanomaterials,
Chemin du Musée 3, CH-1700 Fribourg, Switzerland

²Department of Condensed Matter Physics, Faculty of Science, Masaryk University, Kotlářská 2, 61137 Brno, Czech Republic

³Department of Physics, University of California, San Diego, La Jolla, California 92093, USA

⁴Max-Planck-Institut für Festkörperforschung, Heisenbergstrasse 1, D-70569 Stuttgart, Germany

⁵Karlsruhe Institute of Technology, Institut für Festkörperphysik, D-76021 Karlsruhe, Germany

⁶MacDiarmid Institute, Industrial Research Ltd., P.O. Box 31310, Lower Hutt, New Zealand

We show that a multilayer analysis of the infrared c -axis response of $\text{RBa}_2\text{Cu}_3\text{O}_{7-\delta}$ ($R = \text{Y, Gd, Eu}$) provides important new information about the anomalous normal-state properties of underdoped cuprate high temperature superconductors. In addition to competing correlations which give rise to a pseudogap that depletes the low-energy electronic states below $T^* \gg T_c$, it enables us to identify the onset of a precursor superconducting state below $T^{\text{ons}} > T_c$. We map out the doping phase diagram of T^{ons} which reaches a maximum of 180 K at strong underdoping and present magnetic field dependent data which confirm our conclusions.

The anomalous normal-state properties of underdoped cuprate high temperature superconductors and, in particular, the so-called pseudogap phenomenon remain the subject of an intense debate [1–3]. The wide spectrum of interpretations ranges from a precursor superconducting state (PSC) to electronic correlations that compete with superconductivity (SC). The conflicting experimental data may even be explained in terms of a dual scenario where, as a function of temperature (T), a PSC develops at $T^{\text{ons}} > T_c$ in the presence of a competing pseudogap that depletes the low-energy electronic states below $T^* \gg T^{\text{ons}}$. However, it remains a challenging experimental task to identify these transitions and to disentangle their contributions to the electronic response. In the following we show that this goal can be achieved based on a multilayer analysis of the infrared c -axis conductivity of $\text{RBa}_2\text{Cu}_3\text{O}_{7-d}$ ($R = \text{Y, Gd, Eu}$) single crystals.

Studies of the infrared c -axis conductivity, $\sigma_c(\omega) = \sigma_{1c}(\omega) + i\sigma_{2c}(\omega)$, of underdoped $\text{YBa}_2\text{Cu}_3\text{O}_{7-\delta}$ (Y-123) have shown that besides the so-called spin gap [4], a partial, gaplike suppression also occurs in the low-energy charge excitations [5]. Recent measurements demonstrated that this pseudogap competes with SC, since it removes low-energy spectral weight which is shifted above the gap edge [6]. This is unlike the SC gap at $T < T_c$ where the missing spectral weight is redistributed into a delta function at $\omega = 0$ that accounts for the loss-free response of the SC condensate. The suppression of σ_{1c} at $T > T_c$ thus provides direct information about the T and energy scales, T^* and Δ^{PG} , of the competing pseudogap. Here we outline that the c -axis response of underdoped Y-123 also contains

clear signatures of a PSC state. They are contained in the so-called transverse plasma mode (TPM) and the anomalous T dependence of certain infrared-active phonons which both become most pronounced below T_c but gradually develop already below $T^{\text{ons}} > T_c$ [7–9]. The understanding of these features requires consideration of the layered structure of Y-123 which contains two CuO_2 planes per unit cell (so-called bilayer unit) and the subsequent large difference between the local conductivities inside and outside of these bilayer units, σ_{bl} and σ_{int} , respectively. As a result, the coherent response of the charge carriers gives rise to a mode that is centered at finite frequency, the aforementioned TPM. This is the essence of the so-called multilayer model (MLM) of the c -axis electrostatics [10–12] that quantitatively describes both the TPM and the related phonon anomalies. A remarkable forte of the MLM analysis is in the ability to distinguish and quantify the local conductivities, σ_{bl} and σ_{int} .

$\text{RBa}_2\text{Cu}_3\text{O}_{7-\delta}$ ($R = \text{Y, Gd, Eu}$) crystals of typical dimension $2 \times 2 \times 0.5\text{--}1 \text{ mm}^3$ were grown in Y-stabilized zirconium crucibles as in Ref. [13]. The hole doping of the CuO_2 planes p was adjusted via the oxygen content of the CuO chain layer δ by annealing in flowing O_2 and subsequent rapid quenching. Some strongly underdoped samples were also obtained by partial substitution of R^{3+} with Ca^{2+} [14]. The quoted T_c values were determined by dc magnetization measurements. The p values were obtained either from the measured thermoelectric power (TEP) [14], or from the Ca content with $p = x/2$. The ellipsometric measurements were performed with a home-built ellipsometer attached to a Bruker fast Fourier

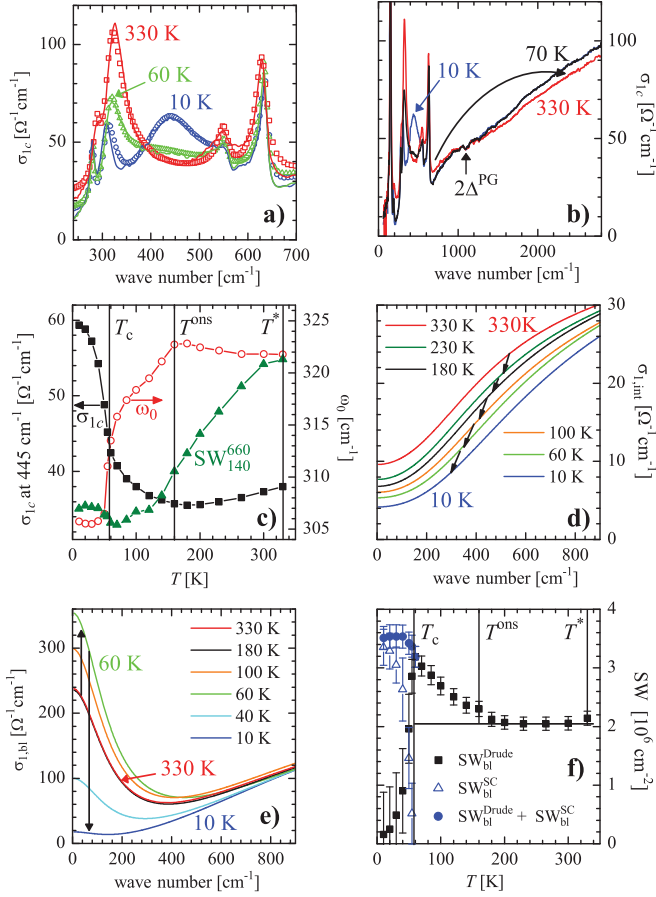


FIG. 1 (color). Multilayer-model analysis of the c -axis response of Y-123 with $T_c = 58$ K. (a) Measured (solid lines) and modeled (symbols) real part of the conductivity σ_{1c} . (b) Expanded scale showing the upwards shift of the SW below $T^* > 300$ K. (c) T dependence of the phonon frequency ω_0 (open circles), the conductivity at the maximum of the TPM (solid squares), and the SW between 140 and 660 cm^{-1} (solid triangles). The latter is replotted with the scale of the vertical axis in Fig. 2(c). (d),(e) Local conductivities of the interbilayer region $\sigma_{1,int}$ and the intrabilayer one $\sigma_{1,bl}$, respectively. (f) T dependence of the SW of the Drude component $\text{SW}_{bl}^{\text{Drude}}$ and of the delta function below T_c , $\text{SW}_{bl}^{\text{SC}}$.

spectrometer below 700 cm^{-1} at the infrared beam line of the ANKA synchrotron at KIT, Germany, and at 400–4000 cm^{-1} with a similar lab-based setup [15]. The presented c -axis polarized spectra are corrected for anisotropy effects using standard numerical procedures. The magnetic field dependence of the c -axis response was measured with a near-normal-incidence reflection and *in situ* gold evaporation technique using the split-coil superconducting magnet at UCSD as described in Ref. [16].

Figure 1 shows the results of the MLM analysis for underdoped $\text{YBa}_2\text{Cu}_3\text{O}_{6.6}$ with $T_c = 58$ (2) K; for details see Ref. [17], part I. Figure 1(a) compares the experimental and fitted spectra of $\sigma_{1c}(\omega)$ and demonstrates that the MLM provides an excellent account of the features that are relevant to the forthcoming discussion, such

as (i) the TPM near 450 cm^{-1} , (ii) the anomaly of the 320 cm^{-1} phonon, and (iii) the suppression of the electronic background by the competing pseudogap with $2\Delta^{\text{PG}} \approx 1100$ cm^{-1} [see Fig. 1(b)]. Their T dependence is detailed in Fig. 1(c) in terms of (i) σ_{1c} (445 cm^{-1}), (ii) the phonon frequency ω_0 , and (iii) the spectral weight (SW) between 140 and 660 cm^{-1} , SW_{140}^{660} . It confirms that the competing pseudogap (iii) appears at a significantly higher temperature of $T^* > 300$ K than the features (i) and (ii) which develop concurrently below $T^{\text{ons}} \approx 160$ K. Figures 1(d) and 1(e) show the real parts of the local conductivities, $\sigma_{1,int}$ and $\sigma_{1,bl}$, as obtained with the MLM. Roughly speaking, $\sigma_{1,int}$ is related to the slowly varying background in $\sigma_{1c}(\omega)$, whereas the information about $\sigma_{1,bl}$ is contained in the TPM and the related phonon anomalies. The low values and the insulatorlike T and frequency dependence of $\sigma_{1,int}$ are characteristic of incoherent transport and reflect the competing pseudogap below $T^* > 300$ K. The important, new information is in $\sigma_{1,bl}$ which contains a sizable Drude-like component that is characteristic of a coherent response. Its T dependence is detailed in Fig. 1(f) in terms of the SW of the Drude component, $\text{SW}_{bl}^{\text{Drude}}$, and of the delta function at $\omega = 0$, $\text{SW}_{bl}^{\text{SC}}$. The latter represents the macroscopically coherent condensate below T_c and has been deduced from $\sigma_{2,bl}$ (not shown). Notably, $\text{SW}_{bl}^{\text{Drude}}$ is not affected at T^* and remains constant down to $T^{\text{ons}} \approx 160$ K below which it starts to increase. Below T_c , the delta function develops and acquires most of the SW. We emphasize that these trends are as expected for a PSC [18]. The increase of $\text{SW}_{bl}^{\text{Drude}}$ below $T^{\text{ons}} \approx 160$ K is caused by a downward shift of SW towards low frequencies, similar to the one that occurs below T_c due to the formation of the SC gap. The response of the partially coherent condensate at $T_c < T < T^{\text{ons}}$ shows up as a Drude-like peak whose width reflects the finite SC correlation time. Below T_c , as these fluctuations are suppressed, all of this SW is finally transferred to the delta function. Note that a markedly different behavior would occur for a spin- or charge density wave state where a significant part of the low-frequency SW would be removed and shifted to higher frequencies.

These observations raise the question of why the signatures of the PSC appear predominantly in $\sigma_{1,bl}$ while that of the competing pseudogap appears mainly in $\sigma_{1,int}$. This is at least partially due to the interbilayer and intrabilayer hopping matrix elements $t_{\perp,int}(\mathbf{k}_{\parallel})$ and $t_{\perp,bl}(\mathbf{k}_{\parallel})$, respectively, and their dependence on the in-plane wave vector \mathbf{k}_{\parallel} . While $t_{\perp,int}(\mathbf{k}_{\parallel})$ is maximal at the boundary of the Brillouin zone (antinodal region) and vanishes along the Brillouin zone diagonal (nodal region), $t_{\perp,bl}(\mathbf{k}_{\parallel})$ depends only weakly on \mathbf{k}_{\parallel} (for details, see Ref. [17], part I). Since the pseudogap is localized in the antinodal region leaving ungapped Fermi arcs in the nodal region [19], $\sigma_{1,int}$ is dominated by the pseudogap while $\sigma_{1,bl}$ contains a major contribution from nodal quasiparticles. This interpretation is supported by the similarity between $\sigma_{1,bl}$ and the in-plane

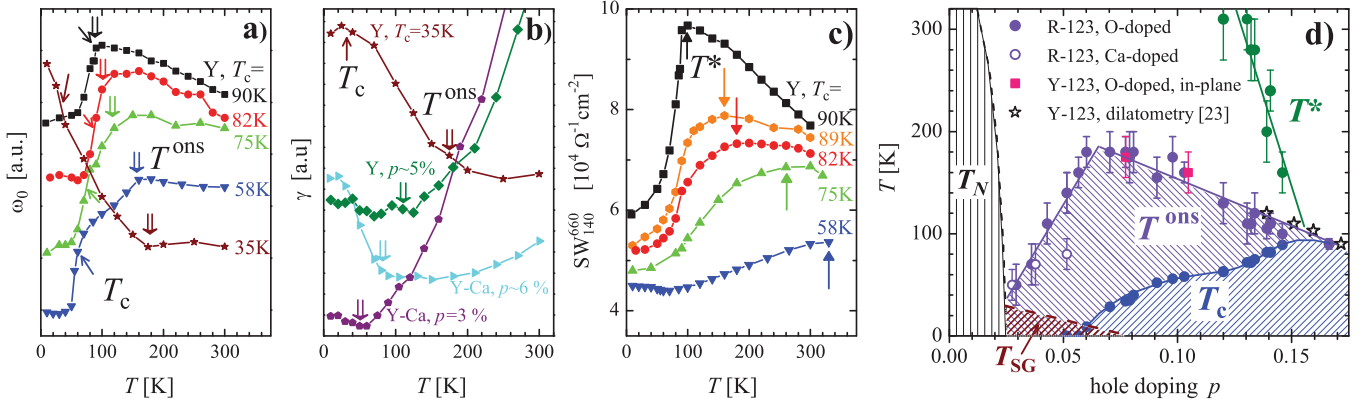


FIG. 2 (color). (a) T dependence of the frequency of the 320 cm^{-1} phonon for $p > 0.08$ shown on a normalized scale. The onset of the anomalous softening at T^{ons} and T_c is marked by thick and thin arrows, respectively. (b) Corresponding changes for $p \leq 0.08$ where T^{ons} is obtained from the anomalous phonon broadening. (c) T dependence of the SW between 140 and 660 cm^{-1} (SW_{140}^{660}) where T^* is determined from the onset of an anomalous decrease as marked by arrows. (d) Resulting doping phase diagram of T^* , T^{ons} , and T_c .

conductivity which also exhibits signatures of the PSC (see Ref. [17], part III).

The scenario of a PSC is furthermore supported by the doping dependence of T^{ons} . The value of T^{ons} has been deduced from the anomalous T dependence of the 320 cm^{-1} phonon mode that coincides with that of the TPM (see Fig. 1(c) and Refs. [9,11]). For $p > 0.08$, we employed the anomalous phonon softening [Fig. 2(a)], while at $p \leq 0.08$, where the TPM merges with the 320 cm^{-1} phonon, we focused on the anomaly in the linewidth γ [Fig. 2(b)]. The corresponding T^* values have been derived from the suppression of SW_{140}^{660} [Fig. 2(c)]. The resulting evolution of T_c , T^{ons} , and T^* is displayed in Fig. 2(d). It highlights that T^{ons} emerges from the T_c line of the overdoped samples and increases on the underdoped side until it reaches a maximum of $T^{\text{ons}} \approx 180 \text{ K}$ close to the boundary of static antiferromagnetism [20,21]. Subsequently, T^{ons} decreases sharply as the metal-to-insulator transition is further approached. The characteristic evolution of T^{ons} , in particular, its domelike shape, is consistent with the assignment to the PCS. It also agrees with previous reports based on Nernst effect and magnetization [22,23], thermal expansion [24], specific heat [25], and recent STM measurements [26]. We emphasize that a fairly large amount of SW is involved in the changes at $T_c < T < T^{\text{ons}}$. The fraction with respect to the changes below T_c grows rapidly on the underdoped side where it exceeds 50% at $T_c = 35 \text{ K}$. Notably, similar trends have been previously derived [22,23] and it was pointed out that these cannot be accounted for by Gaussian fluctuations which would involve a much smaller fraction of electronic states but require critical fluctuations that extend over a wide T range above T_c [27,28]. Note that T^{ons} remains finite even at $3\% < p < 5\%$ where $T_c = 0$. This is likely due to quantum fluctuations which suppress the coherency of the condensate [29].

We also find that the phonon anomalies at $T_c < T < T^{\text{ons}}$, that are directly related to the TPM, can be partially

suppressed with a magnetic field B similar to the behavior below T_c [16]. Figure 3 displays representative spectra of the reflectance ratio, $R_c(B)/R_c(0)$, where B is parallel to the c axis of underdoped Y-123 with $T_c = 58 \text{ K}$, $T^{\text{ons}} \approx 160 \text{ K}$, and $T^* > 300 \text{ K}$ (for details, see Ref. [17], part II). Figure 3(a) shows the 10 K spectra which demonstrate that the strongest feature is associated with the phonon mode at 185 cm^{-1} . This is not surprising since this phonon exhibits large T -dependent changes that are accounted for by the MLM [30] and associated with the intrabilayer currents. Accordingly, it provides a sensitive tool to test whether the magnetic field has a similar effect on the coherency of the electronic state at $T_c < T < T^{\text{ons}}$ as it has at $T < T_c$. That this is indeed the case is shown in Figs. 3(b) and 3(c) where weaker, yet significant and qualitatively similar features appear at 68, 90, and 120 K but are absent at 160 K. We emphasize that this similarity of the magnetic field effects at $T < T_c$ and $T_c < T < T^{\text{ons}}$ is the hallmark of a PCS. Figure 3(d) displays a quantification of the anomaly of the 185 cm^{-1} phonon based on a Lorentz-oscillator fit of the $R_c(8 \text{ T})/R_c(0)$ ratio. The much smaller magnitude of the effect above T_c (than below T_c) can be qualitatively understood as follows. Apart from a partial decoupling of the vortex lines, the large field-induced changes of the TPM and the phonon anomalies at $T \ll T_c$ arise because the vortex cores suppress the volume average of the condensate density of σ_{bl} . This effect is strongly reduced above T_c , where a considerable density of spontaneous vortices and antivortices exists already without the magnetic field whose main effect is likely an increase of the net vorticity. The much weaker field effect above T_c is also consistent with the slower suppression at high fields of the magnetization [23], and the thermal expansion [31].

Next we refer to the corresponding changes in the spin dynamics. The most prominent involves the so-called magnetic resonance mode as measured by inelastic neutron scattering. In optimally doped Y-123 it emerges right below T_c and is recognized as a hallmark of an

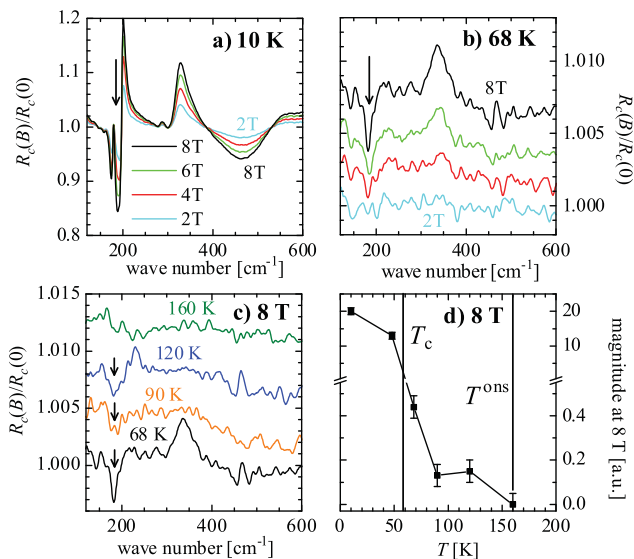


FIG. 3 (color online). (a),(b) Ratio of the c -axis reflectivity in a magnetic field parallel to the c axis, $R_c(B)$, to the one in zero field, $R_c(0)$, of underdoped Y-123 with $T_c = 58$ K. (c) Overview of the 8 T spectra above T_c that are shifted for clarity along the vertical scale. Arrows mark the feature around 185 cm^{-1} . (d) T -dependent magnitude of the feature at 185 cm^{-1} .

unconventional d -wave superconductor [32]. However, for underdoped Y-123 low-energy magnetic excitations persist well above T_c , where they evolve with T in a similar way as the TPM and the phonon anomalies [33,34]. In addition, on some of the same strongly underdoped Y-123 ($T_c = 35$ K) crystals it was recently observed that the spin fluctuations develop a characteristic in-plane anisotropy close to our T^{ons} which has been interpreted in terms of an electronic transition into a nematic liquid state [35]. Such a transition may give rise to a significant enhancement of the pairing correlations [36] and thus explain the fact that our infrared data exhibit a relatively sharp anomaly around T^{ons} even in the strongly underdoped samples.

In summary, we demonstrated that two different correlation phenomena lie at the heart of the anomalous normal-state electronic properties of the underdoped cuprate superconductors. One of them is due to a competing pseudogap that gives rise to an insulatorlike depletion of the density of low-energy electronic states. The other exhibits signatures of a precursor superconducting state since it enhances the spectral weight of the coherent response and is suppressed by a magnetic field. Its onset T reaches a maximum of $T^{\text{ons}} \approx 180$ K in the strongly underdoped regime.

We acknowledge Y.L. Mathis for support at the infrared beam line of the ANKA synchrotron at KIT, D. The work was financed by the Schweizerischer Nationalfonds (SNF) by Grant No. 200020-129484, and the NCCR-MaNEP, the DFG Grant No. BE2684/1 in FOR538, and the Ministry of Education of the CR (MSM002162401). Work at UCSD is supported by NSF and AFOSR.

*christian.bernhard@unifr.ch

- [1] T. Timusk and B. Statt, *Rep. Prog. Phys.* **62**, 61 (1999).
- [2] S. Hühfner, M. A. Hossain, A. Damascelli, and G. A. Sawatzky, *Rep. Prog. Phys.* **71**, 062501 (2008).
- [3] D. N. Basov and T. Timusk, *Rev. Mod. Phys.* **77**, 721 (2005).
- [4] H. Alloul, T. Ohno, and P. Mendels, *Phys. Rev. Lett.* **63**, 1700 (1989).
- [5] C. C. Homes, T. Timusk, R. Liang, D. A. Bonn, and W. N. Hardy, *Phys. Rev. Lett.* **71**, 1645 (1993).
- [6] L. Yu *et al.*, *Phys. Rev. Lett.* **100**, 177004 (2008).
- [7] C. C. Homes, T. Timusk, D. A. Bonn, R. Liang, and W. N. Hardy, *Can. J. Phys.* **73**, 663 (1995).
- [8] J. Schützmann, S. Tajima, S. Miyamoto, Y. Sato, and R. Hauff, *Phys. Rev. B* **52**, 13665 (1995).
- [9] C. Bernhard *et al.*, *Phys. Rev. B* **61**, 618 (2000).
- [10] D. van der Marel and A. Tsvetkov, *Czech. J. Phys.* **46**, 3165 (1996).
- [11] D. Munzar, C. Bernhard, A. Golnik, J. Humlíček, and M. Cardona, *Solid State Commun.* **112**, 365 (1999).
- [12] M. Grüninger, D. van der Marel, A. A. Tsvetkov, and A. Erb, *Phys. Rev. Lett.* **84**, 1575 (2000).
- [13] S. I. Schlachter *et al.*, *Int. J. Mod. Phys. B* **14**, 3673 (2000).
- [14] J. L. Tallon, C. Bernhard, H. Shaked, R. L. Hitterman, and J. D. Jorgensen, *Phys. Rev. B* **51**, 12911 (1995).
- [15] C. Bernhard, J. Humlíček, and B. Keimer, *Thin Solid Films* **455–456**, 143 (2004).
- [16] A. D. LaForge *et al.*, *Phys. Rev. B* **76**, 054524 (2007).
- [17] See supplemental material at <http://link.aps.org/supplemental/10.1103/PhysRevLett.106.047006> for specific details of the data analysis.
- [18] J. Corson *et al.*, *Nature (London)* **398**, 221 (1999).
- [19] K. Tanaka *et al.*, *Science* **314**, 1910 (2006).
- [20] Ch. Niedermayer *et al.*, *Phys. Rev. Lett.* **80**, 3843 (1998).
- [21] S. Sanna, G. Allodi, G. Concas, A. D. Hillier, and R. De Renzi, *Phys. Rev. Lett.* **93**, 207001 (2004).
- [22] Y. Wang, Lu Li, and N. P. Ong, *Phys. Rev. B* **73**, 024510 (2006).
- [23] Lu Li *et al.*, *Phys. Rev. B* **81**, 054510 (2010).
- [24] C. Meingast *et al.*, *Phys. Rev. Lett.* **86**, 1606 (2001).
- [25] J. L. Tallon, J. G. Storey, and J. W. Loram, [arXiv0908.4428v1](https://arxiv.org/abs/0908.4428v1).
- [26] J. Lee *et al.*, *Science* **325**, 1099 (2009).
- [27] V. J. Emery and S. A. Kivelson, *Nature (London)* **374**, 434 (1995).
- [28] Ph. Curty and H. Beck, *Phys. Rev. Lett.* **91**, 257002 (2003).
- [29] V. J. Emery and S. A. Kivelson, *Phys. Rev. Lett.* **74**, 3253 (1995).
- [30] A. Dubroka and D. Munzar, *Physica (Amsterdam)* **405C**, 133 (2004).
- [31] R. Lortz, C. Meingast, A. I. Rykov, and S. Tajima, *Phys. Rev. Lett.* **91**, 207001 (2003).
- [32] B. Keimer *et al.*, *Physica (Amsterdam)* **341C–348C**, 2113 (2000).
- [33] T. Timusk and C. C. Homes, *Solid State Commun.* **126**, 63 (2003).
- [34] V. Hinkov *et al.*, *Nature Phys.* **3**, 780 (2007).
- [35] V. Hinkov *et al.*, *Science* **319**, 597 (2008).
- [36] S. A. Kivelson, E. Fradkin, and V. J. Emery, *Nature (London)* **393**, 550 (1998).